

Supporting information

iRGD-decorated reduction-responsive nanoclusters for targeted drug delivery

Hang Hu ^{a,#}, Jiangling Wan ^{a,b,#}, Xuetao Huang ^{a,#}, Yuxiang Tang ^a, Chen Xiao ^a, Huibi Xu ^{a,b,c},
Xiangliang Yang ^{a,b,c,*}, and Zifu Li ^{a,b,c,d,*}

^aDepartment of Nanomedicine and Biopharmaceuticals, College of Life Science and Technology,
Huazhong University of Science and Technology, Wuhan, 430074, P. R. China

^bNational Engineering Research Center for Nanomedicine, College of Life Science and
Technology, Huazhong University of Science and Technology, Wuhan, 430074, P. R. China

^cHubei Key Laboratory of Bioinorganic Chemistry and Materia Medica, Huazhong University of
Science and Technology, Wuhan, 430074, P. R. China

^dWuhan Institute of Biotechnology, High Tech Road 666, East Lake high tech Zone, Wuhan,
430040, P. R. China

Author Contributions: [#]These three authors contributed equally to this work.

*Corresponding authors:

Professor Zifu Li

Tel.: 86 27 87792234, Fax: 86 27 87792234

E-mail: zifuli@hust.edu.cn

Professor Xiangliang Yang

Tel.: 86 27 87792234, Fax: 86 27 87792234

E-mail: yangxl@hust.edu.cn

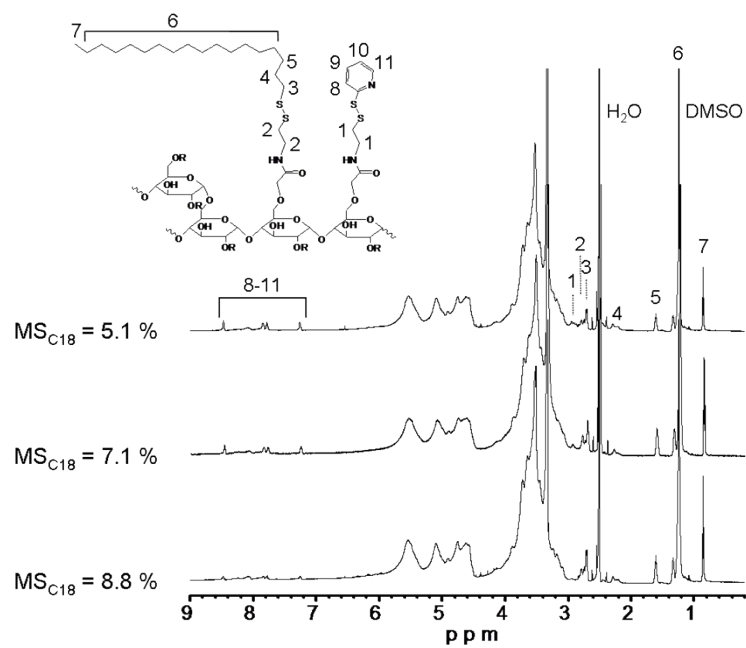


Figure S1. ^1H NMR spectra of HES-SS-C18 with varied MS of C18.

Table S1. Characterization of HES-SS-C18 with varied MS of C18.

Sample	MS_{C18} (%)	MS_{PDA} (%)	Diameter (nm)	PDI
	8.8	1.8	187.7 ± 3.5	0.28 ± 0.05
HES-SS-C18	7.1	3.6	162.3 ± 1.9	0.26 ± 0.02
	5.1	5.3	31.3 ± 9.8	0.26 ± 0.08

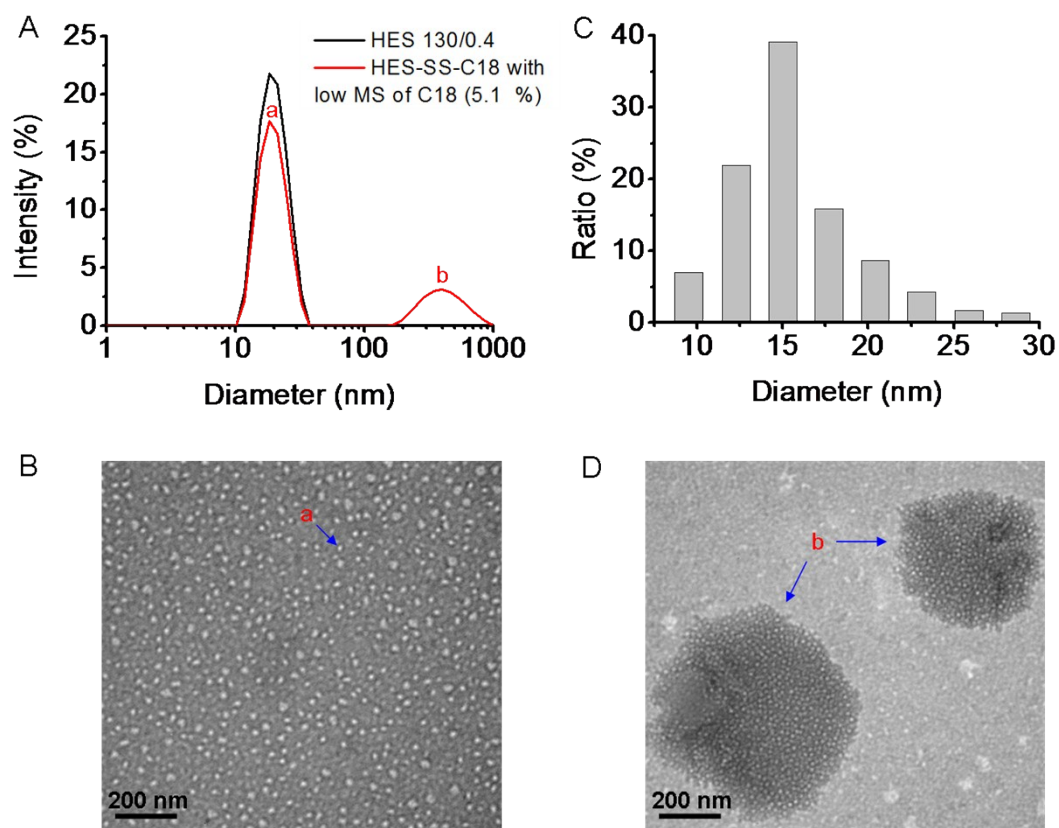


Figure S2. Characterization of HES-SS-C18 with low MS of C18 (5.1 %). (A) Size distribution of HES 130/0.4 and HES-SS-C18 ($MS_{C18} = 5.1\%$) measured by DLS. (B) TEM image of individual HES-SS-C18 ($MS_{C18} = 5.1\%$) nanoparticles. (C) Size distribution of the particles in Figure B. (D) TEM image of large HES-SS-C18 ($MS_{C18} = 5.1\%$) NCs.

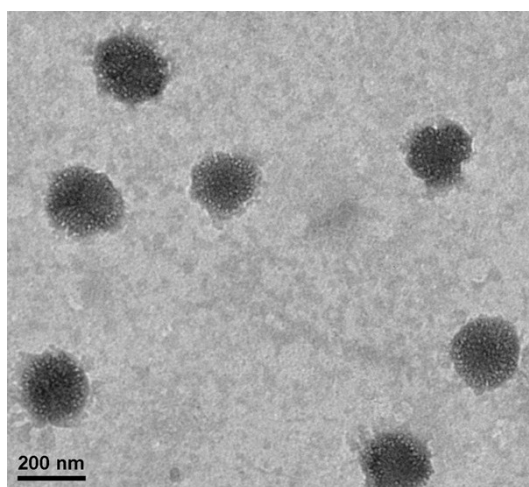


Figure S3. TEM image of HES-SS-C18 NCs with high MS of C18 (8.8 %).

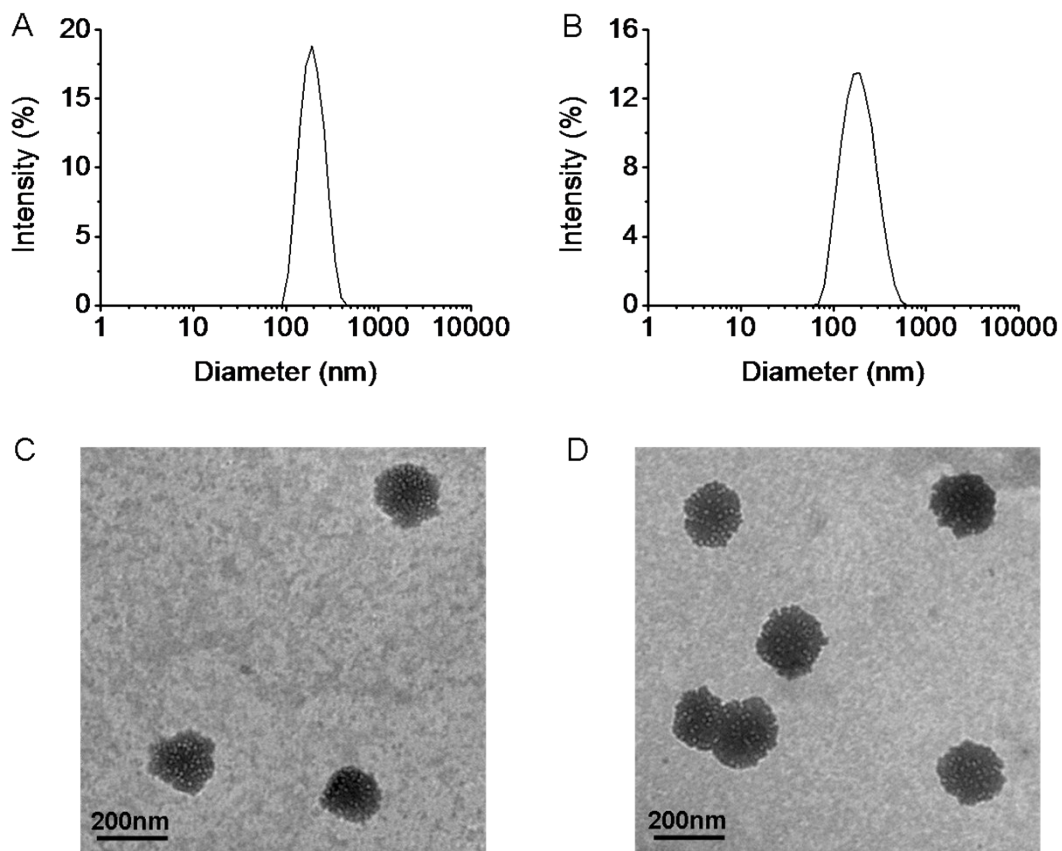


Figure S4. Size and morphology characterization of HES-SS-C18 and iRGD-HES-SS-C18 NCs. (A) Size distribution of HES-SS-C18 NCs measured by DLS. (B) Size distribution of iRGD-HES-SS-C18 NCs measured by DLS. (C) TEM image of HES-SS-C18 NCs. (D) TEM image of iRGD-HES-SS-C18 NCs.

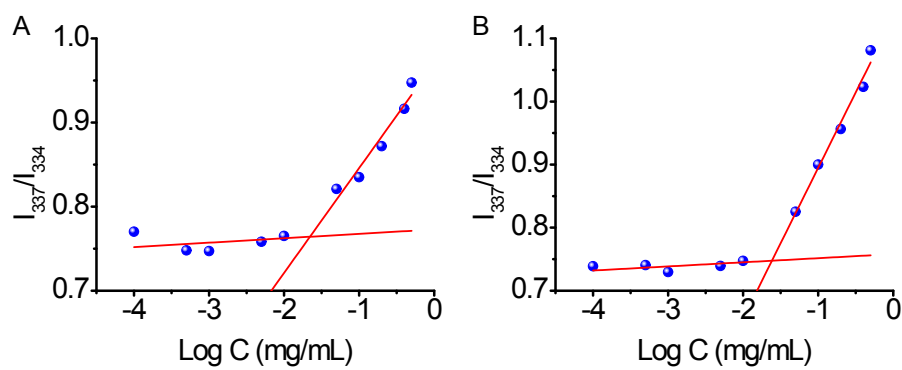


Figure S5. CAC determination of HES-SS-C18 and iRGD-HES-SS-C18. Intensity ratio (I_{337}/I_{334})

of pyrene excitation spectra as a function of log C for HES-SS-C18 (A) and iRGD-HES-SS-C18 (B) in deionized water. The concentration of pyrene was fixed at 6×10^{-7} mol/L.

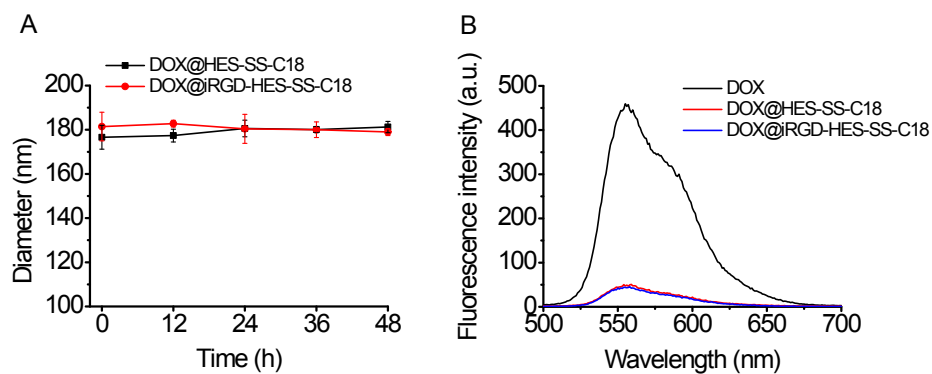


Figure S6. (A) Stability of DOX@HES-SS-C18 and DOX@iRGD-HES-SS-C18 NCs in PBS buffer (pH 7.4, 6.7 mmol/L). (B) Fluorescence spectra of free DOX, DOX@HES-SS-C18 NCs, and DOX@iRGD-HES-SS-C18 NCs (10 μ g/mL as DOX) in PBS buffer (pH 7.4, 6.7 mmol/L). Data represent the mean \pm SD (n = 3).

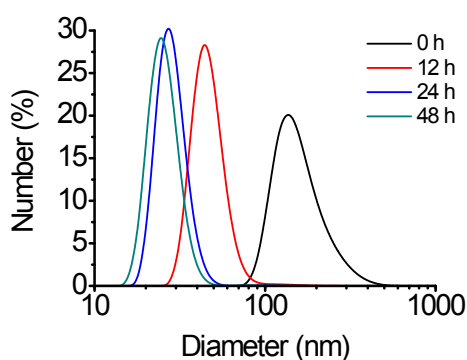


Figure S7. Size changes of DOX@iRGD-HES-SS-C18 NCs after incubation with 20 mmol/L of DTT.

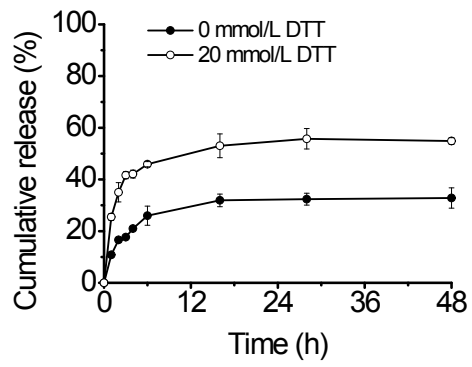


Figure S8. In vitro drug release profiles of DOX@HES-SS-C18 NCs in PBS buffer (pH 7.4, 10.0 mmol/L) with and without 20 mmol/L of DTT.

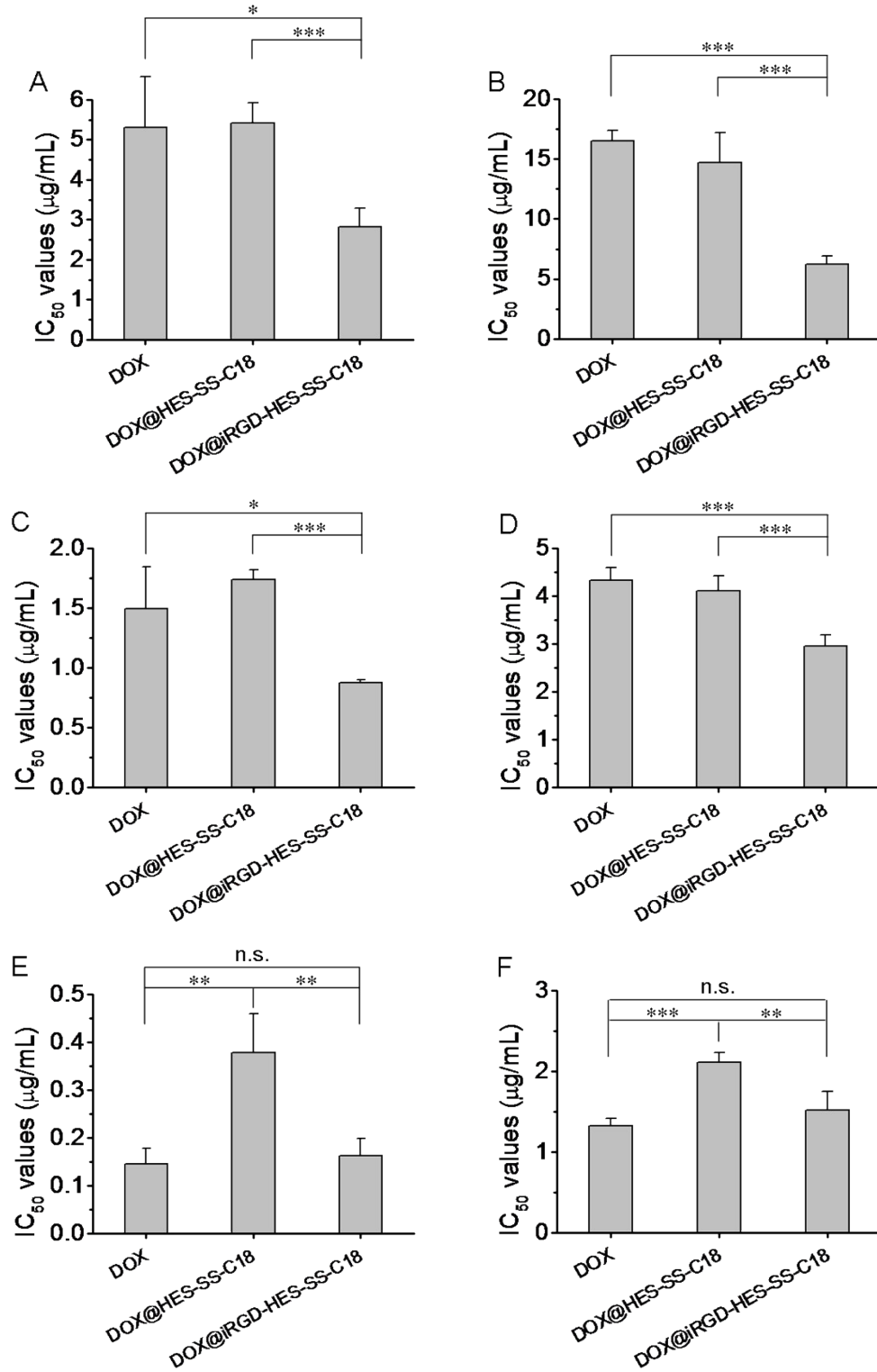


Figure S9. IC₅₀ values of free DOX, DOX@HES-SS-C18 NCs, and DOX@iRGD-HES-SS-C18 NCs against HepG-2 (A, C, E) and 4T1 cells (B, D, F) after incubation for 6 h (A, B), 24 h (C, D), and 48 h (E, F). * $p < 0.05$, ** $p < 0.01$, *** $p < 0.001$. n.s. as not significant. Data represent the mean \pm SD (n = 4).

The in vitro cytotoxicity of DOX-free HES-SS-C18 and iRGD-HES-SS-C18 NCs against HepG-2 and 4T1 cells was evaluated, as shown in Figure S10. The cell viability of HepG-2 and 4T1 cells treated with HES-SS-C18 and iRGD-HES-SS-C18 NCs (from 1 $\mu\text{g}/\text{mL}$ to 1 mg/mL) are all over 90 %, indicating the excellent biocompatibility of our NCs.

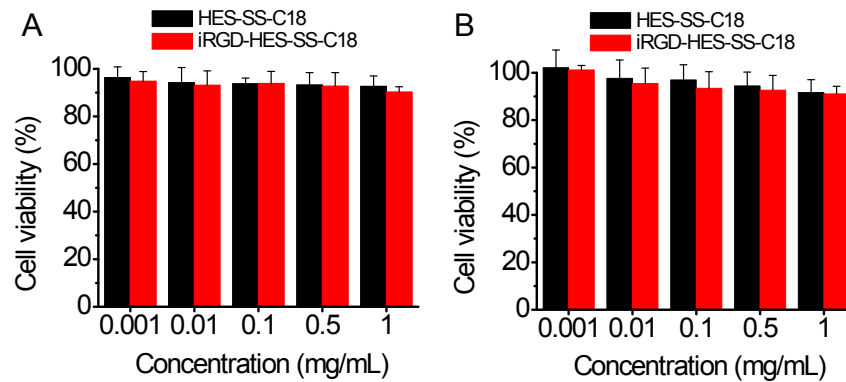


Figure S10. In vitro cytotoxicity of HES-SS-C18 and iRGD-HES-SS-C18 NCs against HepG-2 (A) and 4T1 cells (B). Data represent the mean \pm SD (n = 4).